

Vehicle Charging Observed in SEPAC Spacelab-1 Experiment

Susumu Sasaki,* Nobuki Kawashima,† Kyoichi Kuriki,‡ Masahisa Yanagisawa,§ and Tatsuzo Obayashi¶
The Institute of Space and Astronautical Science, Tokyo, Japan

Electrostatic charging of the orbiter has been studied by the Space Shuttle/Spacelab-1 using the Space Experiments with Particle Accelerators (SEPAC). Charging of the orbiter due to electron beam emission has been analyzed using data from a Langmuir probe, floating probes, an electron energy analyzer and a low-light-level TV camera. Charging of the orbiter is found to be strongly dependent upon the attitude of the orbiter with respect to the velocity vector. The orbiter potential has reached the beam acceleration voltage well beyond one kilovolt, which is much higher than that previously observed in electron beam experiments on sounding rockets in the lower ionosphere.

Introduction

SINCE Hess's first experiment in 1969,^{1,2} high power electron beam experiments in space have been performed extensively for studying beam-plasma and beam-atmosphere interactions³⁻⁷ and also for remote-sensing of electric and magnetic fields in space.^{8,9} One of the important problems in electron beam experiments in space is spacecraft charging because the potential of the spacecraft determines the final beam energy and effective beam power ejected into space. Charging of the spacecraft with weak electron beam emission and without electron beam emission has been studied by satellites.^{10,11} However, for high power electron beam ejection, the information on charging has been very meager in the past experiments.

Theoretical studies of spacecraft charging due to beam ejection have been presented by Beard and Johnson,¹² Parker and Murphy¹³ and Linson.¹⁴ Beard and Johnson have proposed a charging model based on space-charge-limited current where the magnetic field can be neglected. Parker and Murphy's model is an orbital theory for electrons in the magnetic field around the charged body. Linson has suggested a turbulent region surrounding the charged body where the electrons diffuse inward and radially across the magnetic field lines. However, the results of the past rocket experiments with a high power electron beam have entirely disagreed with these models. It has been presumed that charging in the rocket experiments has been much less than predicted by the models.¹⁵ The results of the rocket experiments have been primarily obtained in the lower ionosphere below 200 km. It is of interest to know whether the disagreement between the theoretical models and experiments is also true in the higher ionosphere.

Space Experiments with Particle Accelerators (SEPAC) was carried out by the Spacelab-1 STS-9 mission in 1983.¹⁶ SEPAC was intended to perform an active experiment in space by ejecting a high power electron beam and a high density plasma plume in the ionosphere at an altitude of 250 km. The study of orbiter charging during the beam emission was one of the major objectives of the experiment. Charging of the orbiter while emitting an electron beam of up to 5 kV, 300 mA was observed by onboard diagnostic instruments. This paper presents the results of the analysis of the charging of the orbiter using data from the Langmuir probe, electron energy analyzer, floating probes and low-light-level TV camera.

SEPAC Experiment

The SEPAC onboard instruments were an electron beam accelerator (EBA), magneto-plasma-dynamic arcjet (MPD-AJ), neutral gas plume injector (NGP), TV camera (MTV) and a diagnostic package (DGP). They were configured on the Spacelab pallet as shown in Fig. 1. The shaded instruments belong to SEPAC in the figure. The diagnostic package consists of a Langmuir probe, floating probes, electron energy analyzer, photometer, vacuum gage and VLF (1-10 kHz)/HF (100 kHz + 10 MHz) wave receivers.

During the Spacelab-1 mission, an electron beam up to 5 kV, 300 mA (1.5 kW) was emitted from the orbiter. The duration of the beam emission was either 5 or 1 s. Four experiment sequences (functional objectives: FO-2, -5, -7-1 and -7-2) were performed during night time in different flight configurations. The time chart of the beam firings is shown in Fig. 2 for each FO. In FO-7-1 and 7-2, the plasma plume was also ejected during 1 ms at 0.5 s after the start of the beam emission to study the effect of charge neutralization by the plasma plume.

Results of Analysis

Langmuir Probe Data

A cylindrical probe with an electrode surface of 25 cm² was used as a Langmuir probe, biased from -9 to 9V swept in 84 ms. The change of the probe signal when the beam power is gradually increased is shown for FO-2 in Fig. 3. The current signal modulated by the probe voltage disappears beyond a beam current of 100 mA. There are three types of Langmuir current signal:

- Type 1) Electron current rises from zero at a certain bias voltage.
- Type 2) Electron current modulated by the beam voltage is always positive.
- Type 3) Electron current is always positive and strongly fluctuating (no voltage modulation).

For type 1, the orbiter potential is considered to be less than 9 V and an accurate potential can be calculated from the current onset value. For type 2, the precise potential cannot be calculated, but it must be above 9 V, while not being much higher than the bias voltage. For type 3, the orbiter potential must be well beyond the bias voltage. Type 3 appeared only in FO-2, and Type 1 did not appear in FO-7-2. Type 2 appeared in all FOs. The orbiter potential calculated from the shift of the onset point of the electron current is plotted against the beam current in Fig. 4. The ambiguity of the voltage attributed to the limited resolution of the digitization in the current measurement is 1.6 V at most. Charging is the highest for FO-2 and the lowest for FO-7-1.

The orbiter was charged to a few volts by the lowest beam current of 16 ± 8 mA in FO-2. (The limits are due to the limited resolution in the digitization.) This means that the conductive surface area of the orbiter was effectively less than 30

Received Jan. 5, 1985; revision received March 13, 1985. Copyright © American Institute of Aeronautics and Astronautics, Inc., 1985. All rights reserved.

*Research Associate, Division of Planetary Science.

†Associate Professor, Division of Planetary Science.

‡Professor, Division of Space Propulsion. Member AIAA.

§Research Associate, Division of Space Plasma.

¶Director, Space Plasma Division.

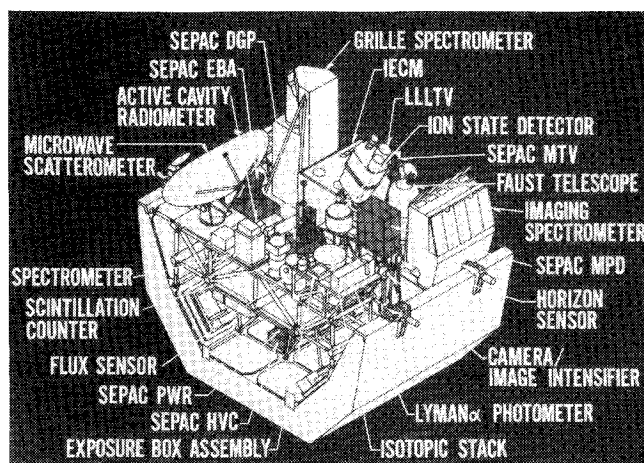


Fig. 1 Configuration of the Spacececlab-1 pallet instruments.

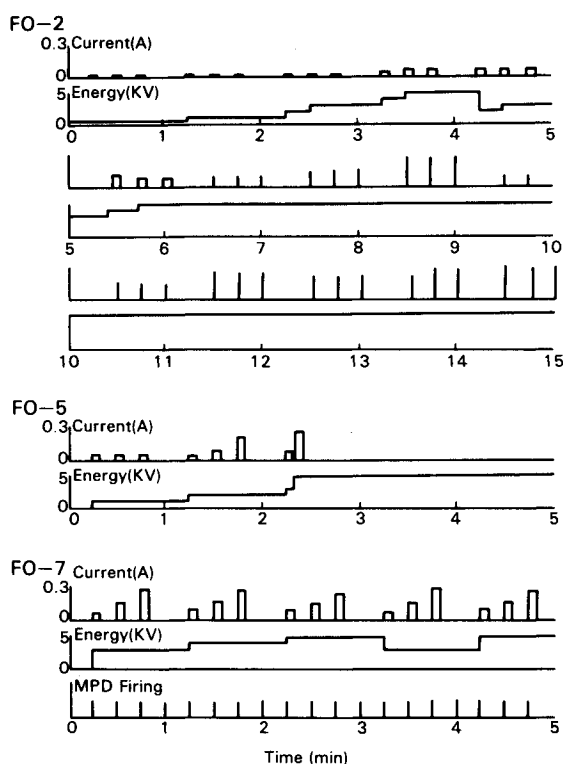


Fig. 2 Sequence chart of electron beam firings.

m^2 in the configuration of FO-2, assuming that the density and temperature of the surrounding plasma were $10^5/cc$ and 1000 K, respectively.

Floating Probe Data

Three cylindrical probes 25 cm apart from each other were mounted on a pole over the deck of the diagnostic package. The surface area of the electrode and the impedance to ground are 50.3 cm^2 and $10 \text{ M}\Omega$, respectively. The output voltage of the probe does not always correspond directly to the orbiter potential. Only qualitative information on charging can be inferred. The typical signal from the floating probe is shown in Fig. 5. As in the case of the Langmuir probe measurement in FO-2, the output voltage increases with the beam current in the low beam current region, and when the beam current exceeds 100 mA, the output voltage starts to fluctuate wildly. The variation of the measurements indicates strong fluctuations in the return current, which is consistent with the Langmuir probe measurement described above.

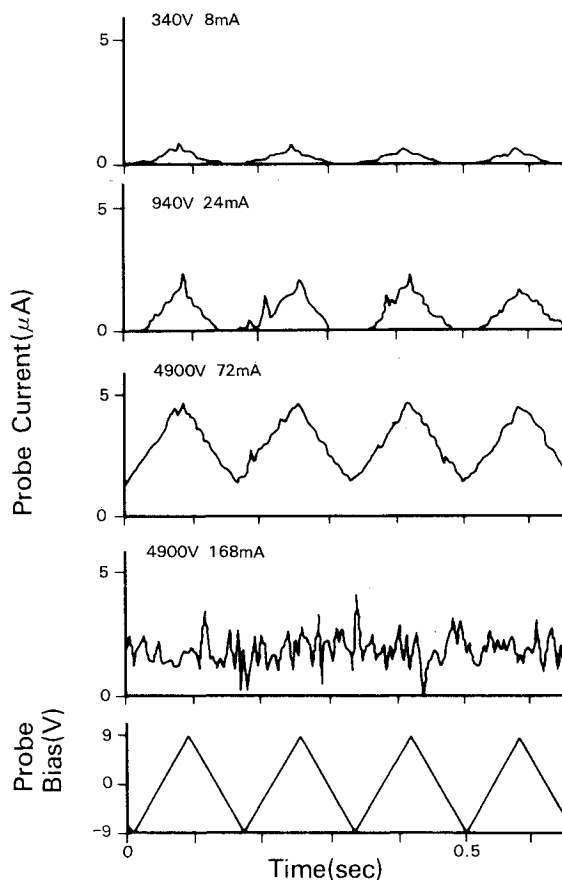


Fig. 3 Langmuir current characteristics when the bias voltage is changed.

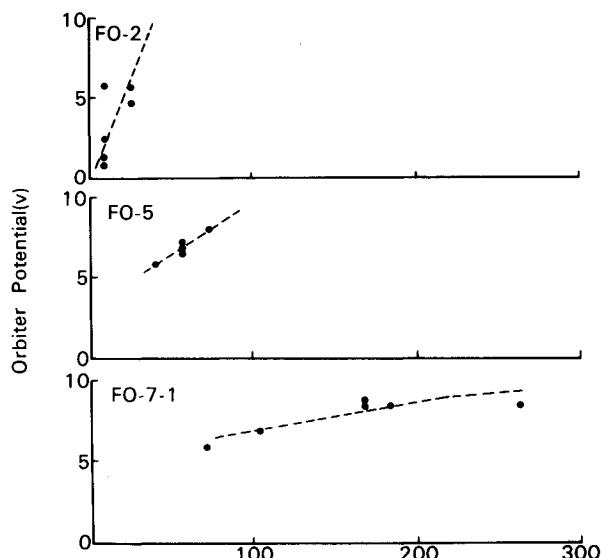


Fig. 4 Potential of the orbiter calculated from the shift of the type 1 Langmuir characteristics.

Electron Energy Analyzer Data

A hemispherical analyzer was used to analyze the incident electron energy from 100 eV to 15 keV. Two types of detectors, the channeltron and the Faraday cup current collector, were employed. The data from the electron energy analyzer is expected to indicate the orbiter potential directly as long as it exceeds 100 V because the peak of the energy spectrum is considered to correspond accurately to the potential of the orbiter which is charged by the electron beam emission.

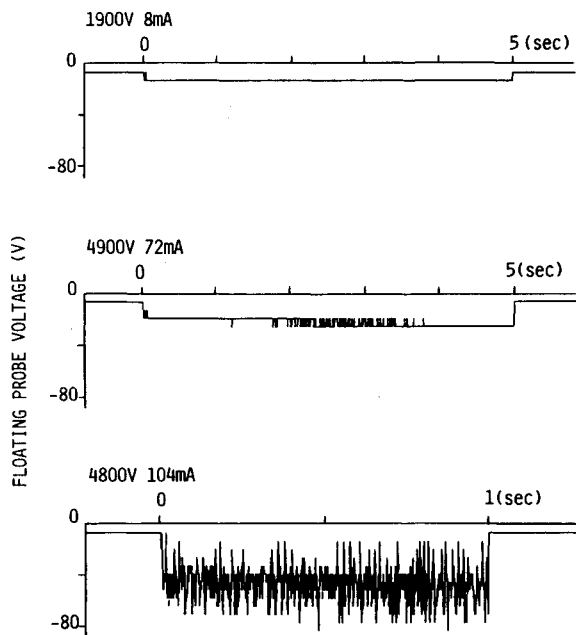


Fig. 5 Change of floating probe signal when the beam current is increased in FO-2.

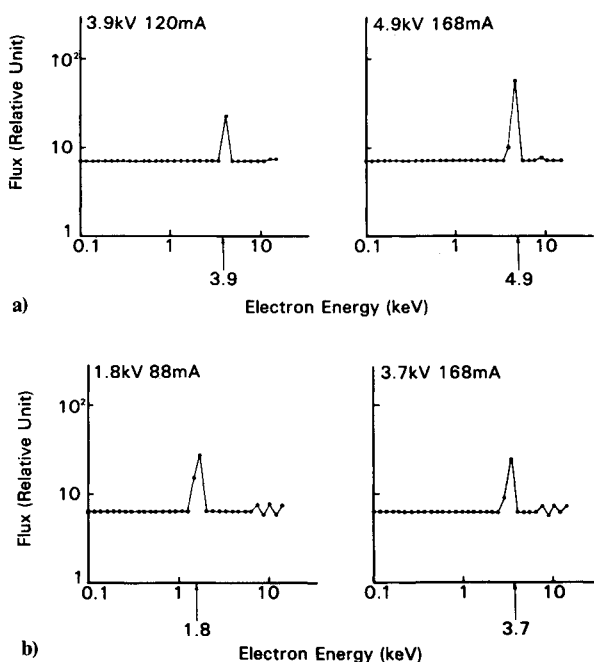


Fig. 6 Examples of electron energy spectra obtained by the Faraday cup detector: a) flight data, b) ground data.

Typical examples of the energy spectrum in FO-2 are shown in Fig. 6a. The peak-structure was detected only when the beam current exceeded 100 mA in FO-2 and the peak of the spectrum corresponded approximately to the beam energy. This means that the orbiter potential reached the beam energy for these cases. Before SEPAC flight hardware was integrated in the Spacelab-1, we had performed a large scale laboratory test using the flight hardware on a simulated pallet in a 8-m diameter space chamber. The simulated pallet together with all control instruments outside the chamber was floating with respect to the chamber wall. A measurement of the charging of the pallet due to the SEPAC electron beam emission was performed. In that experiment, it was possible to measure the

pallet potential with respect to the chamber wall directly and the measured pallet potential could be compared with signals from SEPAC diagnostic instruments. The conclusion was that the energy analyzer with a Faraday cup type current collector can provide correct information on the pallet potential. The same kind of spectrum as in Fig. 6a was obtained in the ground laboratory experiment as shown in Fig. 6b when the simulated pallet was completely charged up to the voltage corresponding to the beam energy.

No single-peak structure in the electron energy spectrum was obtained by the channeltron type detector. The count number seems to be strongly influenced by instrumental effects which must have been caused by the charging of the instrument itself.

TV Camera Data

The low light level TV camera was mounted on a two-axis movable gimbal to follow the beam trajectory. The field of view was $28.7^\circ \times 21.7^\circ$ deg with a fixed focus at 13 m. The sensitivity limit is 10^{-3} lux.

Video data are available only for FO-2 and -5. It is observed that the surface of the instrument was strongly illuminated during beam emissions beyond 100 mA in FO-2 (Fig. 7). On the other hand, no such illumination was detected in FO-5, even when the beam current exceeded 100 mA.

The same illumination of the instruments on the simulated pallet had been observed in the same laboratory experiment in a large space chamber as described in the previous section. In that ground laboratory test, illumination of the instruments was observed when the potential of the simulated pallet with respect to the chamber wall exceeded 1 kV. The light intensity increased with the beam current as well as with the beam voltage. Typical examples obtained during the laboratory experiment, with almost the same beam parameters as those in the SL-1 experiment, are shown in Fig. 8. The high energy electrons, accelerated by the static potential of the charged surfaces, impinge upon the conductive parts over the instruments, exciting the molecules there. The excited light emission irradiates the surroundings. Since the sensitivity of the TV camera was almost the same for both the ground test and flight operation, the orbiter was assumed to be charged above 1 kV when the illumination of the instruments was observed by the TV camera. The beam parameters, when the illumination of the instruments was observed, together with other diagnostic data are shown in Fig. 9 for FO-2. The illumination occurred in coincidence with the appearance of the violent fluctuation in the signals of the Langmuir and floating probes and a sharp peak at the beam energy in the energy analyzer signal.

Discussion

Based on the data from the Langmuir probe, floating probes, electron energy analyzer and the TV camera, the following points about the charging phenomena are concluded.

- 1) FO-2: Charging was the highest. The orbiter potential exceeded 9 V at 24 mA and reached the beam voltage beyond 100 mA.
- 2) FO-5: The orbiter potential exceeded 9 V at 88 mA, but didn't reach the beam voltage even at the maximum current of 280 mA (5 kV).
- 3) FO-7-1: Charging was the lowest. The orbiter potential exceeded 9 V at 280 mA.
- 4) FO-7-2: The orbiter potential exceeded 9 V at the minimum current of 72 mA.

These results are summarized in Fig. 10.

The difference in the charging for each FO can be explained by the difference in the flight configuration of the orbiter. The background plasma density measured by the Langmuir probe was $4 \times 10^3/\text{cc}$ or less for these FOs. Since the probe was located near the bottom of the pallet, the measurements must have been lower than the true background plasma density. The

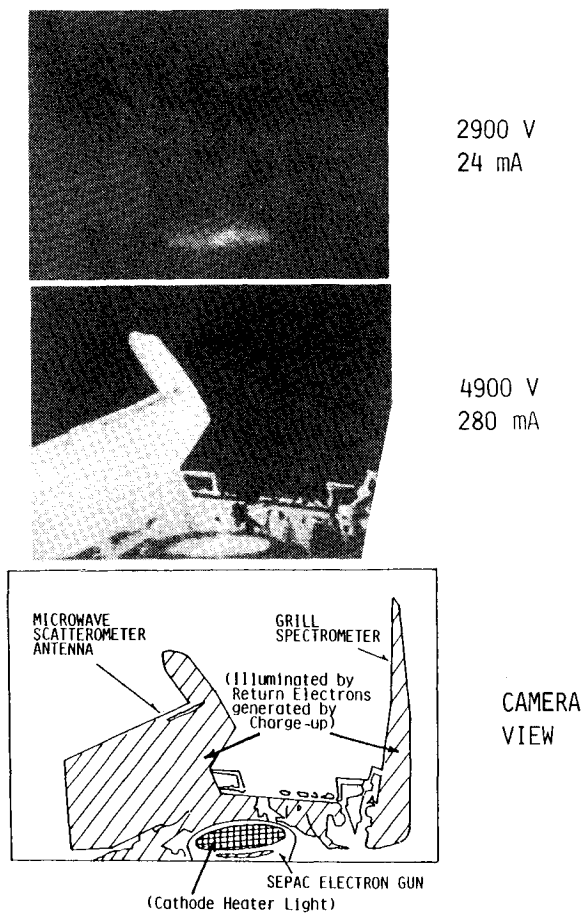


Fig. 7 Illumination of the pallet instruments during the beam emission.

ion density is assumed to be almost constant at approximately $1 \times 10^5/\text{cc}$ because all these FOs were performed during the night.

The conductive surface of the Space Shuttle orbiter is composed of the main engine housing and a lot of small conductive segments distributed over the upper half of the orbiter. The lower portion of the orbiter is completely covered with insulator.

The flight configuration with respect to the velocity vector and geometric field is shown in Fig. 11 for each FO. In the figure, the electron beam was injected approximately along the $-z$ direction. The configuration was almost the same for FO-5 and FO-7-1, in which the potential rise of the orbiter due to the beam emission was comparatively low. In FO-7-1, the potential of the orbiter was less than 9 V even when a beam current of 200 mA was emitted. Since the conductive surface of the main engine housing is less than 30 m^2 , the conductive segments distributed over the orbiter must have played a major role in the current collection. In the FO-2 configuration, the velocity vector of the orbiter was directed downwards to the right wing, while it was directed straight backwards in the other FOs. In the FO-2 configuration, the upper half of the orbiter where the conductive segments are distributed is inside a thick wake, and only the surface of the main engine housing is exposed to the ionospheric plasma. For the other FOs, when the conductive segments are inside a thin wake, the effect of the wake disappears when the orbiter is charged slightly. The electron current from the ionosphere must have hardly been collected by the conductive segments inside the thick wake in the FO-2 configuration. This is the reason why charging was the highest in FO-2. The attitude of the orbiter with respect to the magnetic field also affected the charging of the orbiter. The cross sectional area of the conductive segments on the or-

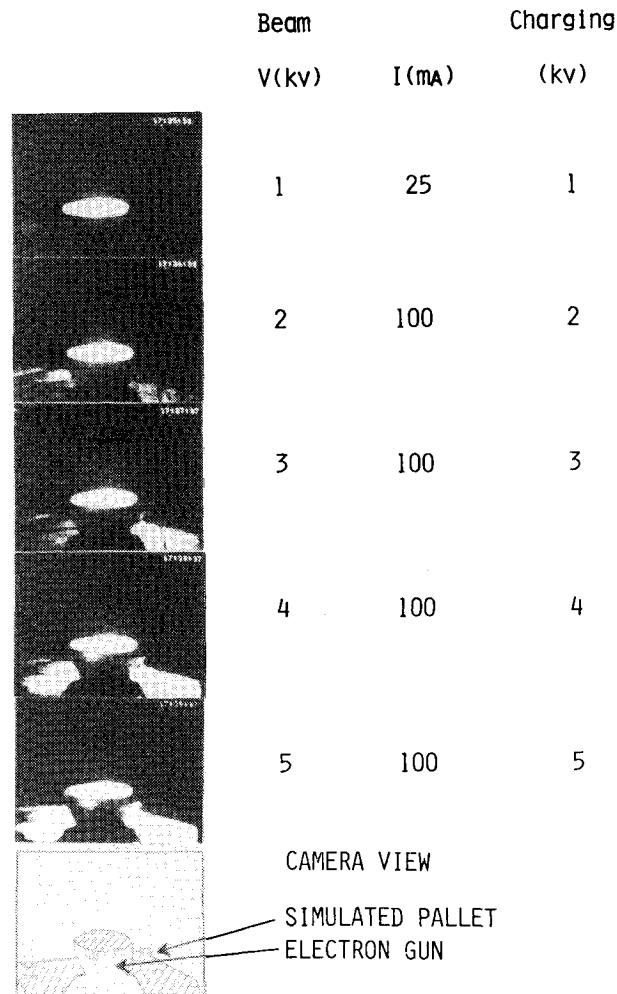


Fig. 8 Illumination of the simulated pallet in a large space chamber.

biter perpendicular to the magnetic field is larger in FO-5 and FO-7-1 than in FO-7-2. Corresponding to this, charging is higher in FO-7-2 than in FO-5 and FO-7-1.

In the past electron beam experiments by sounding rockets in the lower ionosphere, it was generally believed that the spacecraft potential was much smaller than the beam acceleration voltage.¹⁵ The results of the present electron beam experiment show that the potential of the spacecraft reached the beam acceleration voltage when the conductive segments of the orbiter were inside the thick wake. The reasons for the difference between the past rocket experiments and SEPAC experiment are considered to be:

- 1) Rocket experiments have been performed mostly below the height of 200 km, while the SEPAC experiment was carried out at the altitude of 250 km. The plasma production rate surrounding the spacecraft by the beam emission (ionization by primary beam, returning electrons and beam plasma interaction) in the SEPAC experiment must have been relatively smaller because the background gas density is smaller at the orbital height.
- 2) Orbital velocity (7.5 km/s) is much larger than the rocket velocity ($\sim 2 \text{ km/s}$ at most). The conductive surface of the Space Shuttle Orbiter is localized at the upper portion of the orbiter and at the main engine housing, while the surface of the rocket is usually made of conductor. Accordingly, charging depends strongly on the flight configuration with respect to the velocity vector in the case of the Space Shuttle experiment. When the conductive segments get inside the thick wake, charging up to the beam energy begins due to the reduction of the neutralizing plasma effect.
- 3) The rocket is expected to be surrounded by a cloud of outgassed material because the experiment is done only a few

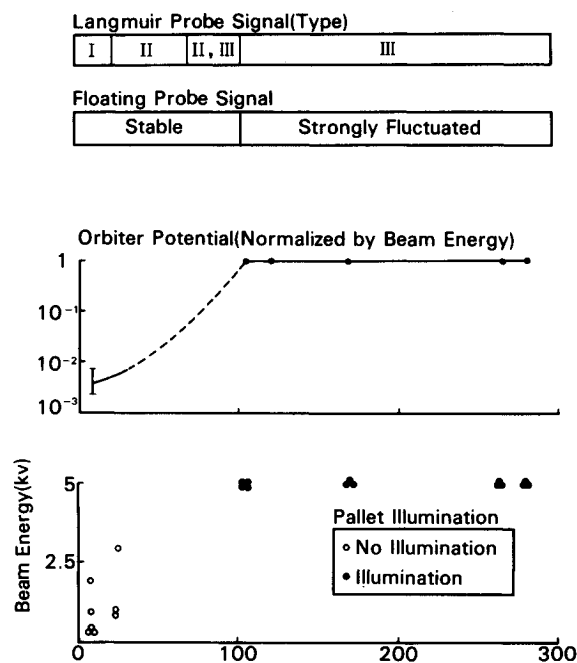


Fig. 9 Parameter region of the electron beam when the pallet instruments are illuminated.

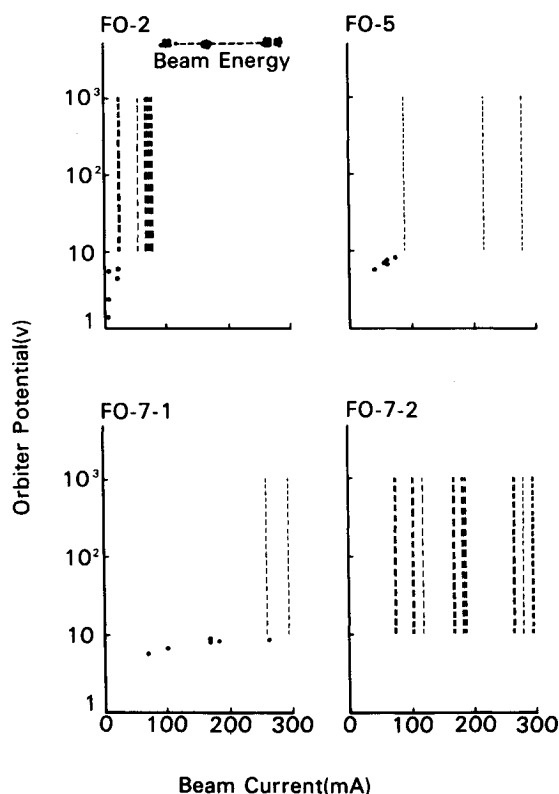


Fig. 10 Potential of the orbiter for each FO. Dotted line means a potential between 9 and 1000 V.

minutes after the surface is exposed to vacuum. The presence of the neutral gas around the rocket is considered to be one of the causes of the creation of the plasma halo around the rocket, which suppresses spacecraft charging.

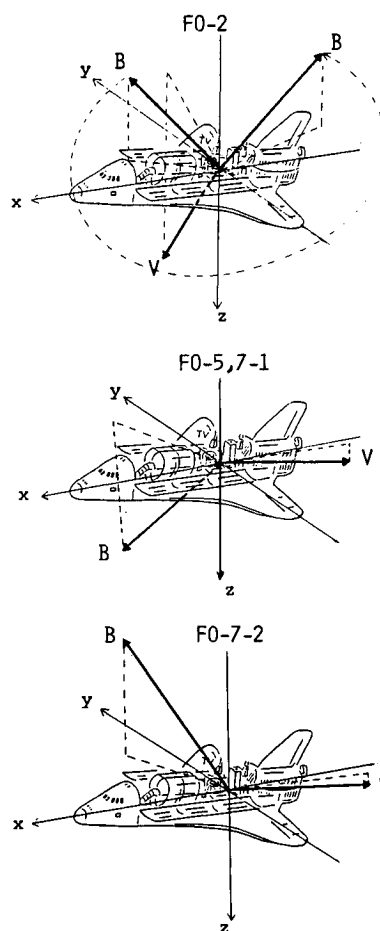


Fig. 11 Flight configuration of the orbiter with respect to the velocity vector (V) and magnetic field (B).

Conclusion

Charging due to electron beam emission in the SEPAC/Spacelab-1 experiment was analyzed. The potential of the orbiter at values less than 9 V was determined using data from the Langmuir probe, and at values beyond 1000 V, the potential was determined using the energy spectrum obtained by the electron energy analyzer. It has been found that the orbiter potential reached the beam voltage beyond one kilovolt when the conductive segments of the orbiter were inside the thick wake, whereas it was much less than one kilovolt when they were located inside the thin wake. These results are qualitatively consistent with the data from the floating probes and TV camera. It can be concluded that charging has been strongly dependent on the flight configuration with respect to the velocity vector in the Spacelab-1 experiment. This was caused by the large Mach number of the orbital speed and the small and localized configuration of the surface of the conductor of the Space Shuttle Orbiter.

Acknowledgment

The authors are very grateful for the collaboration of NASA and ESA Spacelab-1 team members headed by M. H. Craft, Drs. R. Chappell and K. Knott. They also wish to thank Drs. M. Nagatomo, K. Ninomiya, M. Ejiri, I. Kudo and other SEPAC members in promoting the SEPAC project. Thanks are also due to SEPAC co-investigators: Mr. W.T. Roberts and Drs. W.W.L. Taylor, P.R. Williamson, P.M. Banks, D.L. Reasoner, J.L. Burch and O.K. Garriott.

References

- Hess, W.N., Trichel, M.C., Davis, T.N., Beggs, W.C., Kraft, G.E., Stassinopoulos, E., and Maier, E.J.R., "Artificial Aurora Ex-

periment: Experiment and Principal Results," *Journal of Geophysical Research*, Vol. 76, 1971, pp. 6067-6081.

²Davis, T.N., Hallinan, T.J., Mead, G.O., Mead, J.M., Trichel, M.C., and Hess, W.N., "Artificial Aurora Experiment: Ground-Based Optical Observations," *Journal of Geophysical Research*, Vol. 76, Sept. 1971, pp. 6082-6092.

³O'Neil, R.R., Bien, F., Bunt, D., Sandock, J.A., and Stair, A.T. Jr., "Summarized Results of the Artificial Auroral Experiment, Precede," *Journal of Geophysical Research*, Vol. 83, 1978, pp. 3273-3280.

⁴Zhulin, I.A., Markeev, A.K., Mishin, E.V., Ruzhin, Yu.Ya., and Fomichev, V.V., "The High-Frequency Radio Emission Spectral Observations during an Electron Beam Injection into the Ionosphere in the "Zarnitsa-2" Experiment," Academy of Sciences of the USSR Institute of Terrestrial Magnetism, Ionosphere and Radio Wave Propagation, Preprint No. 2 (268) 1980.

⁵Grandal, B., "Highlights of the Observations in the POLAR 5 Electron Accelerator Rocket Experiment," *Artificial Particle Beams in Space Plasma Studies*, edited by B. Grandal, NATO Advanced Study Institutes Series, Series B: Physics Vol. 79, 1982, pp. 159-173.

⁶Kawashima, N., Sasaki, S., Oyama, K., Akai, K., and Nakai, Y., "Floating Potential and Return Current Measurements in a Rocket-Borne Electron Beam Experiment," *Geophysical Research Letters*, Vol. 9, 1982, pp. 1061-1063.

⁷Banks, P.M., Raitt, W.J., Williamson, P.R., White, A.B., and Bush, R.I., "Results from the Vehicle Charging and Potential Experiment on STS-3," submitted to AIAA *Journal of Spacecraft and Rockets*, 1984.

⁸Hendrickson, R.A., McEntire, R.W., and Winckler, J.R., "Echo I: An Experimental Analysis of Local Effects and Conjugate Return

Echoes from an Electron Beam Injected into the Magnetosphere by a Sounding Rocket," *Planetary Space Science*, Vol. 23, 1975, pp. 1431-1444.

⁹Winckler, J.R., Arnold, R.L., and Hendrickson, R.A., "Echo 2: A Study of Electron Beams Injected into the High-Latitude Ionosphere from a Large Sounding Rocket," *Journal of Geophysical Research*, Vol. 80, 1975, pp. 2083-2088.

¹⁰Kawashima, N., and the JIKIKEN (EXOS-B) CBE Project Team, "Wave Excitation in Electron Beam Experiment on Japanese Satellite 'JIKIKEN (EXOS-B),'", *Artificial Particle Beams in Space Plasma Studies*, edited by B. Grandal, NATO Advanced Study Institutes Series, Series B: Physics Vol. 79, 1982, pp. 101-110.

¹¹Olsen, R.C. and Purvis, C.K., "Observations of Charging Dynamics," *Journal of Geophysical Research*, Vol. 88, July 1983, pp. 5657-5667.

¹²Beard, D.B. and Johnson, F.S., "Ionospheric Limitations on Attainable Satellite Potential," *Journal of Geophysical Research*, Vol. 66, Dec. 1961, pp. 4113-4122.

¹³Parker, L.W. and Murphy, B.L., "Potential Buildup on an Electron-Emitting Ionospheric Satellite," *Journal of Geophysical Research*, Vol. 72, March 1967, pp. 1631-1636.

¹⁴Linson, L.M., "Current-Voltage Characteristics of an Electron-Emitting Satellite in the Ionosphere," *Journal of Geophysical Research*, Vol. 74, 1969, pp. 2368-2375.

¹⁵Winckler, J.R., "The Application of Artificial Electron Beams to Magnetospheric Research," *Review of Geophysical Space Physics*, Vol. 18 1980, pp. 659-682.

¹⁶Obayashi, T. et al., "Space Experiments with Particle Accelerators," *Science*, Vol. 225, 4658, 1984, pp. 195-196.

From the AIAA Progress in Astronautics and Aeronautics Series

THERMOPHYSICS OF ATMOSPHERIC ENTRY—v. 82

Edited by T.E. Horton, The University of Mississippi

Thermophysics denotes a blend of the classical sciences of heat transfer, fluid mechanics, materials, and electromagnetic theory with the microphysical sciences of solid state, physical optics, and atomic and molecular dynamics. All of these sciences are involved and interconnected in the problem of entry into a planetary atmosphere at spaceflight speeds. At such high speeds, the adjacent atmospheric gas is not only compressed and heated to very high temperatures, but strongly reactive, highly radiative, and electronically conductive as well. At the same time, as a consequence of the intense surface heating, the temperature of the material of the entry vehicle is raised to a degree such that material ablation and chemical reaction become prominent. This volume deals with all of these processes, as they are viewed by the research and engineering community today, not only at the detailed physical and chemical level, but also at the system engineering and design level, for spacecraft intended for entry into the atmosphere of the earth and those of other planets. The twenty-two papers in this volume represent some of the most important recent advances in this field, contributed by highly qualified research scientists and engineers with intimate knowledge of current problems.

Published in 1982, 521 pp., 6×9, illus., \$35.00 Mem., \$55.00 List

TO ORDER WRITE: Publications Dept., AIAA, 1633 Broadway, New York, N.Y. 10019